

# Optics Letters

## Cost-effective fiber-to-lithium niobate chip coupling using a double-side irradiation self-written waveguide

LIANGJUN HE,  HANKE FENG, CHENG WANG,  AND HAU PING CHAN\* 

Department of Electrical Engineering, City University of Hong Kong, 83 Tat Chee Avenue, Kowloon Tong, Hong Kong SAR, China

\*Corresponding author: eehpchan@cityu.edu.hk

Received 2 November 2022; revised 8 December 2022; accepted 9 December 2022; posted 12 December 2022; published 2 January 2023

In recent years, integrated lithium niobate (LN) chips have been widely used for developing a variety of photonic devices, such as high-speed electro-optical (EO) modulators and frequency comb generators. A major challenge for their practical applications is the high coupling loss between micrometer-scale LN waveguides and optical fibers. Lensed fibers and special taper structures are commonly used to tackle the coupling issue. However, in some situations, these approaches may increase the overall complexity and cost of design, fabrication, and alignment. Here, we propose using the self-written waveguide (SWW), an optical waveguide induced by light irradiation, to cope with this coupling issue. The approach can apply in connecting a single-mode fiber (SMF) to any waveguide surface in principle, even with a large mode-field mismatch, significantly alleviating the tight alignment requirements typically needed for end-fire coupling into integrated waveguides. Our study demonstrates that the coupling loss between a SMF with a mode-field diameter (MFD) of  $4.4\text{ }\mu\text{m}$  and a sub-micrometer LN rib waveguide could be dramatically reduced from an initial value of  $-14.27\text{ dB}$  to  $-5.61\text{ dB}$ , after double-side irradiated SWW formation. Our proposed approach offers a potential solution for achieving a cost-effective and flexible fiber-to-LN chip optical interconnect. © 2023 Optica Publishing Group

<https://doi.org/10.1364/OL.479820>

Lithium niobate (LN) has received considerable attention in advanced photonics due to its attractive optical properties like high optical nonlinearity, good electro-optical (EO) modulation ability, a wide optical transparency window, and high refractive index contrast. With the development of nanofabrication technology, thin-film lithium niobate-on-insulator (LNOI) has been applied in many nanophotonic devices to achieve significant optical functionalities, including high-speed EO modulation [1–7], supercontinuum generation [8], Kerr frequency comb generation [9,10], and second harmonic generation [11,12]. However, there is a severe coupling issue with integrating LN waveguides and optical fibers. When they are butt-coupled, significant coupling loss occurs due to the large mode-field mismatch caused by the size and geometric difference. Due to the difficulty in deep dry etching and design constraints in EO modulation, integrated LN waveguides typically feature a vertically

asymmetric rib structure, which substantially differs from the geometry of optical fibers. With the high coupling loss, the optical power delivered to the chips is compromised, ultimately restricting the performances of individual devices and whole photonic systems.

Several methods have been adopted to cope with the coupling issue mentioned above. Firstly, one could apply lensed fibers to substitute conventional optical fibers for coupling with integrated LN waveguides. To a certain extent, the method can reduce the initial coupling loss by using the smaller mode-field of lensed fibers to match the mode-field of integrated LN waveguides more easily [13]. However, lensed fibers are not very commercially significant due to their small tolerance in alignment and sensitivity to environmental fluctuations. Other designs, including grating couplers [14–16] and mode size converters [13,17,18], are proposed to improve the coupling efficiency further. However, the grating coupler approach is narrowband in nature, whereas using mode size converters requires bilayer tapers on the integrated LN rib structures, which may raise the design and fabrication complexity. Therefore, a flexible and cost-effective method to reduce the coupling loss between optical fibers and integrated LN chips is highly desirable.

In this Letter, we propose using the self-written waveguide (SWW) approach for the first time to address the coupling issue between optical fibers and integrated LN chips. The SWW approach creates an optical waveguide in photo-curable epoxy by irradiating suitable laser light directly from the optical structures to be coupled (e.g., fibers, waveguides). This optical waveguide, once formed, will act as a low-loss optical link between the cores of optical devices. The approach has many advantages, including easy fabrication, high mechanical strength, low optical coupling loss, and good alignment tolerance [19]. Compared with other methods, it is a flexible and cost-effective way to solve coupling issues.

To form SWWs in silicon photonics, two-photon absorption (TPA) is usually required due to the non-transparency of silicon over the visible spectrum [20–22]. In contrast, LN material exhibits excellent transparency in visible bands, making it possible to form SWWs using direct irradiation of a visible light source. In our study, we cured dye-doped epoxy using green light irradiation to create an SWW between a single-mode fiber (SMF) with a mode-field diameter (MFD) of  $4.4\text{ }\mu\text{m}$  and a sub-micrometer LN rib waveguide. Both single-side irradiation and

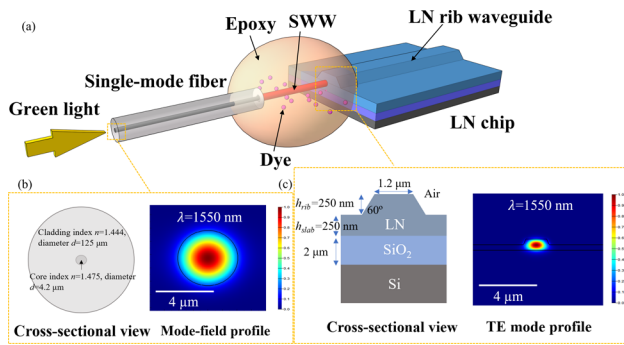


**Fig. 1.** (a) Schematic diagram of the SWW formed between an SMF and an LN chip; (b) cross-sectional view and mode-field profile of the SMF; (c) cross-sectional view and TE mode profile of the LN waveguide.

double-side irradiation conditions were investigated. The initial coupling loss is  $-14.27\ \text{dB}$ , measured under direct contact between the SMF and the LN waveguide. In the case of double-side irradiation, after forming an SWW between the fiber and the LN rib waveguide, the measured coupling loss is reduced to  $-5.61\ \text{dB}$ . Our findings offer great potential for efficient coupling between optical fibers and sub-micrometer LN chips with asymmetric structures.

Firstly, we need to choose a suitable combination of dye and epoxy materials to facilitate our investigation. We applied MasterBond UV11-3 as the epoxy due to its optical transparency, wide range of service temperatures ( $-50^\circ\text{C}$  to  $120^\circ\text{C}$ ), and relatively low viscosity (60 centipoises). As for dyes, we used Rhodamine 6 G (R6G), the most common xanthene dye [full compound name: (9-(*o*-(ethoxycarbonyl)phenyl)-6-ethylamino-2,7-dimethyl-3-xanthenylidene) ethyl ammonium chloride]. It has an absorption peak at a wavelength ( $\lambda$ ) of around 530 nm. Therefore, we used a common green laser source at 532 nm to irradiate R6G and form the SWW by photo-polymerization [19].

Figure 1(a) illustrates the schematic diagram of the proposed SWW formed between an SMF and an LN chip. The SMF employed in our experiment is a high numerical aperture fiber ( $\text{NA} = 0.29$ ) with an MFD of  $4.4\ \mu\text{m}$ . We used finite-difference-time-domain (FDTD) simulation to investigate the mode-field distributions of the SMF and the LN rib waveguide at a wavelength of  $1550\ \text{nm}$  ( $n_{\text{LN}} = 2.14$ ,  $n_{\text{SiO}_2} = 1.444$ ). As is shown in Fig. 1(c), the top rib LN waveguide is around  $1.2\ \mu\text{m}$  in width with a height  $h_{\text{rib}}$  of  $250\ \text{nm}$  (rib waveguide angle  $\sim 60^\circ$ ). The height of the slab layer  $h_{\text{slab}}$  is  $250\ \text{nm}$  as well. The whole LN thin film is on top of  $2\text{-}\mu\text{m}$ -thick silicon dioxide on a silicon substrate. The LN waveguide supports a fundamental transverse-electric (TE) optical mode with an MFD of around  $1.5\ \mu\text{m}$ . In this study, we try to address the significant mode-field mismatch between the SMF and the LN waveguide issue using an SWW, aiming to reduce the high coupling loss that ultimately affects the device's performance.

We applied a micropositioner to control the location of the SMF and pre-align it with the LN waveguide. Based on our experience managing large-mode mismatch issues, we chose an air gap of  $\sim 30\ \mu\text{m}$  between them to be filled with dye-doped epoxy and form the SWW [19]. Green light at  $532\ \text{nm}$  was launched into the dye-doped epoxy through the SMF, which is absorbed by R6G and induces a photo-polymerization process that increases the local refractive index. As the index change rises monotonically with the light intensity, the most vigorous

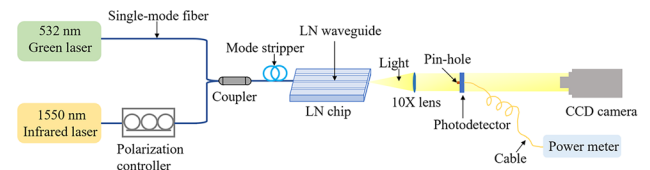


**Fig. 2.** Schematic diagram of the experimental setup. First, a CCD camera monitors the LN waveguide output light profile to align the optical path. Then the CCD camera is replaced by a photodetector with a power meter to measure the  $1550\text{-nm}$  output power from the LN waveguide.

light intensity near the center of the fiber core leads to a high-index SWW core that can effectively confine and guide the light [23]. In this way, the SWW was formed between the cores of the SMF and the LN waveguide. The formed SWW can provide an optical link that effectively guides light transmitting from the SMF to the LN waveguide.

The experimental characterization setup is depicted in Fig. 2. Stabilized green laser light ( $\lambda=532\ \text{nm}$ ) and an infrared laser ( $\lambda=1550\ \text{nm}$ ) were launched together by a coupler into the LN waveguide via the SMF (MFD  $\sim 4.4\ \mu\text{m}$ ). We employed a polarization controller after the infrared laser to ensure TE polarization. The telecom SMF supports several high-order modes at green wavelength, which may affect the formation of the SWW. Therefore, a mode stripper was placed before the LN waveguide to eliminate high-order modes of green light. The green light was used to form an SWW between the SMF and the LN waveguide, while the infrared laser was used to monitor the coupling loss between them in real time. The output light was collected using a  $10\times$  objective lens and observed using a charge-coupled device (CCD) camera for optical alignment. Then the CCD camera is replaced by a photodetector with a power meter to measure the  $1550\ \text{nm}$  output power from the LN waveguide. We set a pinhole before the photodetector to block undesired stray light to collect mainly the fundamental mode of the LN rib waveguide.

We demonstrate the successful fabrication of SWWs between the cores of the SMF and the LN rib waveguide by applying the experimental setup and materials (dye and epoxy) discussed above. The effects of different parameters on the loss-reduction performance of the formed SWW were investigated. In the case of single-side irradiation where green light transmits through dye-doped epoxy from the SMF to the LN waveguide, we observed that it took approximately 15 minutes to form an SWW with 0.5 percentage weight (%-wt) dye concentration and  $1.36\ \text{mW}$  green light illumination. Figure 3(a) depicts the

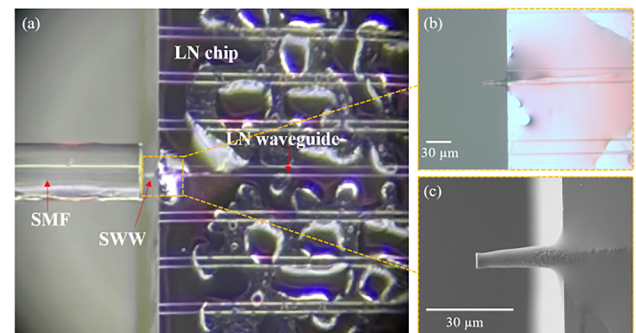


**Fig. 3.** (a) Microscopic image of the SWW formed between the SMF and the LN waveguide; zoom-in (b) optical microscopic and (c) SEM images of the SWW connected to the LN waveguide.

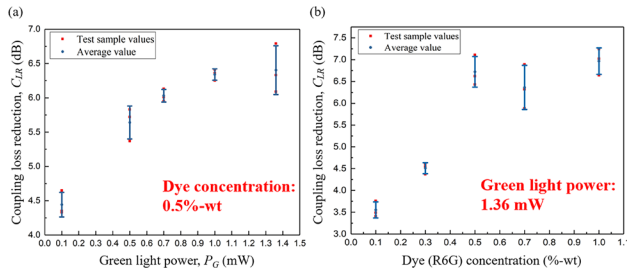


**Fig. 4.** (a) Coupling loss reduction between the SMF and the LN waveguide under different green light powers; (b) coupling loss reduction between the SMF and the LN waveguide under different dye concentrations.

microscopic image of the SWW formed between the SMF and the LN waveguide. Here we removed the surrounding epoxy of the SWW using acetone to better view the formed SWW structure. To further obtain a detailed view of the SWW, we carefully broke the SWW away from the SMF and inspected the SWW using an optical microscope [Fig. 3(b)] and a scanning electron microscope (SEM) [Fig. 3(c)]. It can be seen from Fig. 3(c) that a waveguide-like SWW structure is formed connecting the core of the LN waveguide, facilitating light transmission from the SMF to the LN waveguide. The waveguide structure, once formed, will not disappear even when the light source is removed. It will act as an optical link and effectively guide the light transmitting from the SMF to the LN waveguide.

We investigated the effects of the photo-polymerization parameters on the performance of the SWW during the process. The first parameter is the green light power ( $P_G$ ), which needs to be large enough to initiate the photo-polymerization process. Another parameter that needs to be studied is the R6G dye concentration, which is associated with the photon absorption and curing process when green light irradiates. During the process of our study, we employed the control variable method. First, we fixed the dye concentration at 0.5%-wt, and applied different powers of green light to irradiate the dye-doped epoxy to form the SWW between the SMF and the LN waveguide. Then we used our experimental setup to measure the coupling loss reduction ( $C_{LR}$ ) between them. Similarly, we maintained a constant irradiating green light power of 1.36 mW for dye-doped epoxy materials with different dye concentrations (0.1, 0.3, 0.5, 0.7, and 1.0%-wt). After the formation of the SWW under the conditions mentioned above, the  $C_{LR}$  values were measured and illustrated in Fig. 4.

Figure 4(a) illustrates the performance of the SWW formed under different green light power intensities (i.e., 0.1, 0.5, 0.7, 1.0, and 1.36 mW) in reducing the coupling loss between the SMF and the LN waveguide. When the green light power is low (0.1 mW), the coupling loss reduction ( $C_{LR}$ ) between the SMF and the LN waveguide is relatively small, only 4.4 dB. With an increase in green light power,  $C_{LR}$  becomes more significant, indicating a better coupling efficiency between the SMF and the LN waveguide. The intrinsic mechanism of this phenomenon is that when the green light power is low, there is insufficient energy to accomplish the photo-polymerization process fully. In this case, some dye molecules cannot absorb and interact with photons, which affects the quality of the formed SWW. The quality of the SWW determines the coupling efficiency between the SMF and the LN waveguide. When the green light power increases beyond a certain value, the  $C_{LR}$  no longer increases but tends to be saturated at 6.4 dB, which is limited by the dye

concentration. Under this condition, no more dye molecules are available to interact with the increased photons, which may not help form the SWW anymore. Thus, coupling loss reduction cannot be further improved.

To further improve the coupling performance and better match the high index contrast of the LN waveguide, we prepared and tested several concentrations of dye-doped epoxy materials for SWW formation. Figure 4(b) illustrates the coupling loss reduction between the SMF and the LN waveguide at different dye concentrations. When the dye concentration is low (0.1%-wt),  $C_{LR}$  is not impressive, only around 3.5 dB. Under this circumstance, although there is sufficient light intensity to initiate the photo-polymerization process, the number of dye molecules is too small. During the formation of the SWW, the refractive index increase is not significant enough to match the index contrast of the LN waveguide. Therefore, the coupling efficiency between the SMF and the LN waveguide is low. With the increase of dye concentration, the refractive index increase becomes more significant, leading to a larger  $C_{LR}$ . The loss reduction performance sees saturation behavior at high dye concentrations. This is because when the green light power remains constant and does not increase, the interactions between dye molecules and photons tend to be saturated. As a result, the uncured dye molecules cannot absorb photons to further increase the refractive index contrast. Thus, the  $C_{LR}$  and the coupling efficiency cannot be improved anymore.

From the above analysis, green light power and dye concentration are two critical parameters dominating the SWW formation process. They are interactional and mutually restricted. The green light power is responsible for initiating the photo-polymerization process while increasing the dye concentration improves the refractive index contrast. We can further reduce the coupling loss between the SMF and the LN waveguide by optimizing these two parameters. The initially measured fiber-to-chip coupling loss is -14.27 dB. After the formation of the SWW with a single-side irradiation power of 1.36 mW and a 0.5%-wt dye concentration, the coupling loss is reduced by 6.56 dB, indicating that our approach can effectively reduce the coupling loss between fiber and LN chip.

To further improve the coupling efficiency between the SMF and the LN waveguide, we applied a double-side irradiation method to fabricate the SWW. An optical coupler was used to simultaneously launch the green light from the LN waveguide and the SMF side. We also used mode strippers placed in front and at the back of the LN chip to eliminate high-order modes of the green light. In this case, the SWW will grow both from the LN waveguide and the SMF end during the photo-polymerization process. The schematic diagram is shown in Fig. 5.

We fabricated an SWW between the LN waveguide and the SMF under 1.36 mW green light power and 0.5%-wt dye concentration using this double-side irradiation scheme. The measured fiber-to-chip coupling loss improves from -14.27 dB to -5.61 dB ( $C_{LR} \sim 8.66$  dB) at the wavelength of 1550 nm. The improved  $C_{LR}$  is due to a better mode matching than the single-side irradiation condition. Since we irradiated green light from both the SMF and the LN waveguide, the initially grown SWW structures are more consistent with the SMF and LN waveguide modes. Therefore, this method can effectively reduce the coupling loss between the SMF and the LN waveguide. However, this method requires more precise alignment and higher operation requirements. The launching angle of the green light needs to be adjusted precisely. Besides, the green light may generate high-order modes



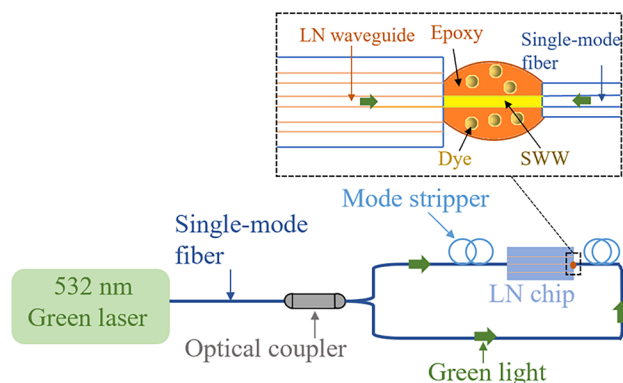


**Fig. 5.** Schematic diagram of the SWW formation process between the LN waveguide and the SMF under double-side irradiation conditions.

during transmission in the LN waveguide, which also affects the formation of SWW. Indeed, we could further optimize our experimental procedures and parameters (e.g.,  $P_G$  and dye concentration) to improve the coupling efficiency between the SMF and the LN chip under double-side and single-side illumination conditions, respectively.

In conclusion, we have proposed and demonstrated experimentally applying an SWW to reduce the substantial coupling loss between optical fibers and integrated LN chips. The SWW was realized by irradiating green light on dye-doped epoxy using both single-side and double-side irradiation to induce a photopolymerization process. We investigated two critical parameters ( $P_G$  and dye concentration) that dictated the SWW formation process and offered insights into their relationships. After the formation of the SWW under the double-side irradiation condition, the measured fiber-to-chip coupling loss is reduced from an initial value of  $-14.27$  dB by  $8.66$  dB to  $-5.61$  dB. This approach can reduce the significant coupling loss between optical fibers and integrated LN chips cost-effectively without a complex design and nanofabrication process. The high coupling efficiency offers possibilities for the optical interconnecting between LNOI devices and paves the way for widespread applications in optical communications and sensing based on LN-integrated photonics. The present work also provides a potential solution to interface photonic chips in different material platforms and with varying spot sizes.

**Funding.** City University of Hong Kong (9220024).

**Acknowledgment.** Supported by the Donation Research Grant of the City University of Hong Kong (9220024).

**Disclosures.** The authors declare no conflicts of interest.

**Data availability.** Data underlying the results presented in this paper are not publicly available at this time but may be obtained from the authors upon reasonable request.

## REFERENCES

1. M. Jin, J. Chen, Y. Sua, P. Kumar, and Y. Huang, *Opt. Lett.* **46**, 1884 (2021).
2. S. Sun, M. He, M. Xu, X. Zhang, Z. Ruan, L. Zhou, L. Liu, L. Liu, S. Yu, and X. Cai, *J. Lightwave Technol.* **39**, 1108 (2021).
3. C. Wang, M. Zhang, B. Stern, M. Lipson, and M. Lončar, *Opt. Express* **26**, 1547 (2018).
4. P. O. Weigel, J. Zhao, K. Fang, H. Al-Rubaye, D. Trotter, D. Hood, J. Mudrick, C. Dallo, A. T. Pomerene, A. L. Starbuck, C. T. DeRose, A. L. Lentine, G. Rebeiz, and S. Mookherjea, *Opt. Express* **26**, 23728 (2018).
5. A. J. Mercante, S. Shi, P. Yao, L. Xie, R. M. Weikle, and D. W. Prather, *Opt. Express* **26**, 14810 (2018).
6. M. R. Escalé, D. Pohl, A. Sergeyev, and R. Grange, *Opt. Lett.* **43**, 1515 (2018).
7. M. He, M. Xu, Y. Ren, J. Jian, Z. Ruan, Y. Xu, S. Gao, S. Sun, X. Wen, and L. Zhou, "High-performance hybrid silicon and lithium niobate Mach-Zehnder modulators for 100 Gbit/s and beyond," *arXiv*, arXiv:1807.10362 (2018).
8. M. Yu, B. Desiatov, Y. Okawachi, A. L. Gaeta, and M. Lončar, *Opt. Lett.* **44**, 1222 (2019).
9. C. Wang, M. Zhang, R. Zhu, H. Hu, and M. Lončar, "Monolithic photonic circuits for Kerr frequency comb generation, filtering and modulation," *arXiv*, arXiv:1809.08637 (2018).
10. Y. He, Q. F. Yang, J. Ling, R. Luo, H. Liang, M. Li, B. Shen, H. Wang, K. Vahala, and Q. Lin, "A self-starting bi-chromatic LiNbO<sub>3</sub> soliton microcomb," *arXiv*, arXiv:1812.09610 (2018).
11. R. Luo, H. Jiang, S. Rogers, H. Liang, Y. He, and Q. Lin, *Opt. Express* **25**, 24531 (2017).
12. C. Wang, C. Langrock, A. Marandi, M. Jankowski, M. Zhang, B. Desiatov, M. M. Fejer, and M. Lončar, *Optica* **5**, 1438 (2018).
13. L. He, M. Zhang, A. Shams-Ansari, R. Zhu, C. Wang, and M. Lončar, *Opt. Lett.* **44**, 2314 (2019).
14. Z. Chen, R. Peng, Y. Wang, H. Zhu, and H. Hu, *Opt. Mater. Express* **7**, 4010 (2017).
15. I. Krasnokutska, R. J. Chapman, J.-L. J. Tambasco, and A. Peruzzo, *Opt. Express* **27**, 17681 (2019).
16. B. Chen, Z. Ruan, X. Fan, Z. Wang, J. Liu, C. Li, K. Chen, and L. Liu, *APL Photonics* **7**, 076103 (2022).
17. Y. Li, T. Lan, J. Li, and Z. Wang, *Appl. Opt.* **59**, 6694 (2020).
18. G. Yang, A. V. Sergienko, and A. Ndao, *Opt. Express* **29**, 18565 (2021).
19. L. He, H. P. Chan, and B. Li, *Opt. Express* **29**, 36745 (2021).
20. H. Terasawa, F. Tan, O. Sugihara, A. Kawasaki, D. Inoue, T. Yamashita, M. Kagami, O. Maury, Y. Bretonnière, and C. Andraud, *Opt. Lett.* **42**, 2236 (2017).
21. F. Tan, H. Terasawa, O. Sugihara, A. Kawasaki, T. Yamashita, D. Inoue, M. Kagami, and C. Andraud, *J. Lightwave Technol.* **36**, 2478 (2018).
22. A. Barsella, H. Dorkenoo, and L. Mager, *Appl. Phys. Lett.* **100**, 221102 (2012).
23. T. Yamashita, M. Kagami, and H. Ito, *J. Lightwave Technol.* **20**, 1556 (2002).